Available online at www.sciencedirect.com
ScienceDirect
Journal of Sound and Vibration 299 (2007) 621–632
JOURNAL OF SOUND AND VIBRATION
www.elsevier.com/locate/jsvi

# Bifurcation and chaos response of a cracked rotor with random disturbance

Xiaolei Leng[a,*], Guang Meng[b], Tao Zhang[c], Tong Fang[d]

[a]*Institute of Vibration Engineering Research, College of Aerospace Engineering, Nanjing University of Aeronautics and Astronautics, Nanjing 210016, PR China*
[b]*The State Key Lab of Vibration, Shock and Noise, Shanghai Jiao Tong University, Shanghai 200240, PR China*
[c]*The Third Institute, China Aerospace Science and Industry Corp., Beijing 100074, PR China*
[d]*Department of Mechanics, Northwest Ploytechnical University, Xi'an 710072, PR China*

Received 12 November 2004; received in revised form 25 April 2006; accepted 10 July 2006
Available online 9 October 2006

**Abstract**

The Monte-Carlo method is used to investigate the bifurcation and chaos characteristics of a cracked rotor with a white noise process as its random disturbance. Special attention is paid to the influence of the stiffness change ratio and the rotating speed ratio on the bifurcation and chaos response of the system. Numerical simulations show that the affect of the random disturbance is significant as the undisturbed response of the cracked rotor system is a quasi-periodic or chaos one, and such affect is smaller as the undisturbed response is a periodic one.


## 1. Introduction

The dynamic behavior of a cracked rotor is of great importance to rotor crack detection. Up till now, many characteristics of a cracked rotor have been revealed, for example, unstable speed range near rotating speed $\omega = 2\omega_c/N$, where $\omega_c$ is the first pin–pin critical and $N = 1, 2, 3, 4$ [1]; large influence of crack position on system's dynamic response [2]; and variation of response amplitude and phase angle with crack [3]. But all of these conclusions were based on the linear crack model, and weight dominance was assumed in almost all the analyses of horizontal cracked rotor and the influence of whirl speed on the closing and opening of crack was omitted. Meng and Gasch [4] analyzed the nonlinear influence of whirl speed. The angle between the crack center line and the line connecting the bearing and shaft center was used for determining the closing and opening of the crack, so the crack model is nonlinear and includes the cases with and without weight dominance, synchronous and non-synchronous responses. This nonlinear crack model is used in this paper, and the system's equations of motion are nonlinear ones with time-varying coefficients.

Random disturbance is often encountered in some rotor machines, such as the electric generators service in seismic zone, and the power-generating machine of an oceangoing ship. Thus, there is a need for analyzing the

*Corresponding author. Tel.: +86 25 84892106.
*E-mail address:* lengxl@nuaa.edu.cn (X. Leng).

0022-460X/$ - see front matter © 2006 Elsevier Ltd. All rights reserved.
doi:10.1016/j.jsv.2006.07.006

**Nomenclature**

| | | | |
|---|---|---|---|
| $D_e$ | external damping ratio | $T$ | dimensionless time ($=\omega t$) |
| $k_0$ | stiffness of uncracked shaft | $\omega$ | rotating speed |
| $\Delta K$ | stiffness change ratio | $\omega_c$ | pin–pin critical speed of uncracked rotor |
| $m$ | mass of rotor | $\omega_{cr}$ | pin–pin critical speed of cracked rotor |
| $U$ | dimensionless unbalance parameter | $\omega_r$ | whirl speed (non-synchronous rotating speed relative to synchronous one) |
| $X$, $Y$ | dimensionless deflection | $\Omega_c$ | critical speed ration ($\omega_{cr}/\omega_c$) |
| $\beta$ | the angle between crack and unbalance | $\Omega$ | rotating speed ration ($\omega/\omega_c$) |
| $\xi, \eta$ | body fixed rotating coordinates, $\xi$ is the crack direction | $\varphi_0$ | initial phase of unbalance |
| | | $\gamma(t)$ | a standard white noise process |
| | | $\sigma$ | intensity of random disturbance |

response problem of a rotor system subject to random disturbances. Zhao and Lin [9] used direct integration scheme in the analysis of the rotor bearing systems subjected to random earthquake excitation. But in their research, the rotor model is assumed to be a linear one, and the crack's influence was not taken into account. In this paper, the rotor system mentioned above with a white noise process as its random disturbance is investigated numerically. And our particular focus is on the affect of the random disturbance on bifurcation and chaos character of the system, which will likely be utilized in the future fault diagnosing of rotating machinery.

## 2. Mathematical model

For the simple Jeffecott rotor with a transverse crack is subject to a random disturbance, taking whirl speed $\omega_r$ into account, supposing the cross stiffness change ratio caused by rotor crack to be zero (Fig. 1), and using the nonlinear crack model derived by Meng and Gasch [4], the non-dimensional equations of motion can be written as follows:

$$\begin{Bmatrix} \ddot{X} \\ \ddot{Y} \end{Bmatrix} + \frac{2D_e}{\Omega}\begin{Bmatrix} \dot{X} \\ \dot{Y} \end{Bmatrix} + \frac{1}{\Omega^2}\begin{Bmatrix} X \\ Y \end{Bmatrix} - \frac{\Delta K \cdot f(\Psi)}{2\Omega^2}\begin{bmatrix} 1+\cos 2\Phi & \sin 2\Phi \\ \sin 2\Phi & 1-\cos 2\Phi \end{bmatrix}\begin{Bmatrix} X \\ Y \end{Bmatrix} = \begin{Bmatrix} 1/\Omega^2 \\ 0 \end{Bmatrix} + U\begin{Bmatrix} \cos\tau \\ \sin\tau \end{Bmatrix} + \sigma\gamma(t)\begin{Bmatrix} 1 \\ 0 \end{Bmatrix}, \tag{1}$$

where $\Phi = \tau + \beta + \varphi_0$, $\Psi = \Phi - \arctan(Y/X)$, $f(\Psi) = \frac{1}{2} + (2/\pi)\cos\Psi - (2/3\pi)\cos 3\Psi + (2/5\pi)\cos 5\Psi$.

Suppose that $\sigma\gamma(t)$ in Eq. (1) is the random disturbance of the rotor system, with $\gamma(t)$ as a standard white noise process, and constant $\sigma > 0$ as the intensity of the random disturbance.

Eq. (1) is a nonlinear one with time varying coefficients, disturbed with a white noise process. In this paper, we take $\Omega$ and $\Delta K$ as varying parameters, and use a four-step Runge-Kutta method to integrate Eq. (1). To illustrate the numerical result, those tools, such as orbit diagram, Poincare map and bifurcation diagram are used.

Monte Carlo method can be used in numerical analysis of dynamics response of nonlinear structure subject to random excitations. In its approach, a random process can be simulated as a series of cosine function with

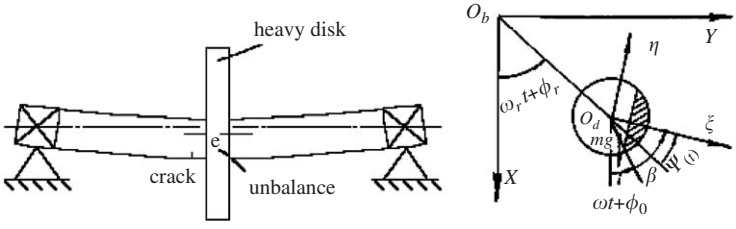


Fig. 1. Schematic diagram of a nonlinear cracked rotor.

weighted amplitudes and random phase angles. This approach was presented by Shinozuka in 1970s firstly [7,8]. With a few simple modifications, some similar approaches can be used in the numerical analysis of (a) wind-induced ocean wave elevation, (b) spatial random variation of material properties, (c) random surface roughness of highways and airport runways. In this paper, we suppose that $\gamma(t)$ is a standard white noise process, which can be simulated as

$$\gamma(t) = 2\sqrt{\frac{S \cdot \omega_0}{N}} \sum_{k=1}^{N} \cos\left[k\frac{\omega_0}{N}t + \theta_k\right]. \tag{2}$$

Here, $N$ is a large integral number, $\omega_0$ is the truncation frequency in the simulation of $\gamma(t)$, $\theta_k$ $(k = 1, 2, \ldots, N)$ are mutually independent random variables distributed between 0 and $2\pi$, and $s = 1.0$ presents spectral density of a standard white noise process, $\gamma(t)$. If $\theta_k$ take a series of deterministic values, namely $\tilde{\theta}_k$, where $\tilde{\theta}_k \in [0, 2\pi]$, the corresponding $\tilde{\gamma}(t)$ obtained from Eq. (2) will be a sample process of the white noise process $\gamma(t)$. The process simulated in this method will be an ergodic one as $N \to \infty$, and the simulated spectral density converges as $1/\sqrt{N}$ in the mean square sense to the target spectral density [7,8]. In the following simulation, $N$ and $\omega_0$ are taken as 500 and 25, respectively.

## 3. Results and discussion

As the rotor crack will decrease the rotor stiffness, the pin–pin critical speed of cracked rotor is smaller than that of the uncracked rotor. Therefore, the critical speed ratio $\Omega_c < 1$ for cracked rotor, and $\Omega_c = 1$ for uncracked system. Most of the response of the rotor system without random disturbance is omitted here to economize the paper, while some related results are presented in Appendix A.

Fig. 2 shows the influence of $\Delta K$ on the response of the rotor system subject to a white noise process, when $\beta = 0$, $u = 0.1$ and $\Omega$ is near to $2/3\Omega_c$ ($\Omega = 0.6$). Here bifurcation diagrams corresponding to a gradual increase of stiffness change ratio $\Delta K$ of the system response are shown in Fig. 2(a) (for the intensity of the random disturbance $\sigma = 0.001$) and Fig. 2(b) (for $\sigma = 0.01$), respectively; Fig. 2(c) and (d) are orbit diagrams of the system response corresponding to $\Delta K = 0.35$, respectively, where (c) for $\sigma = 0.001$ and (d) for $\sigma = 0.01$; Fig. 2(e) and (f) are power spectrum diagrams corresponding to 2(c) and (d), respectively; Fig. 2(g) and (h) are Poincare diagrams of the system response corresponding to $\Delta K = 0.5$, where (g) for $\sigma = 0.001$ and (h) for $\sigma = 0.01$; and Fig. 2(i) and (j) are power spectrum diagrams corresponding to 2(g) and 2(h).

From the bifurcation diagram, Fig. 2(a), we can see that the bifurcation curves just turn a little thicker; and the bifurcation value of parameter $\Delta K$ is almost invariant, compared to the curves while the rotor system is not disturbed. But as we can see in Fig. 2(b), the bifurcation curves are thicker than those in Fig. 2(a), moreover, the bifurcation process cannot be distinguished clearly when $0.534 < \Delta K < 0.55$. That is to say, the influence of $\sigma\gamma(t)$ on the response of the rotor system is very weak when its intensity, $\sigma$, is a little one; and such influence grows intensive as $\sigma$ increases. From Fig. 2(c) and (d), we can find that the orbit diagrams corresponding to $\Delta K = 0.35$ turn to be a family of unclosed curves. And the profile of those unclosed curves is similar to the corresponding periodical solution curves of the undisturbance system. In this study, such solution is named as the random disturbed periodical solution. Furthermore, the difference between Fig. 2(c) and (d) shows that the disturbed periodical solution of the rotor system fluctuates according to the increase of $\sigma$. From the Poincare diagram of the system, Fig. 2(g) and (h) corresponding to $\Delta K = 0.5$, we can see that some similar phenomena occur. In this case, the solution of the disturbed rotor system is named as random disturbed quasi-periodical solution. In other words, here the Poincare diagram comes to be a series of discrete points distributing round a closed curve because of the effect of random disturbance, which represents quasi-periodic solutions of the undisturbed system. And along with the increase of $\sigma$, the distribution of those discrete points turns more dispersed. From the power spectrum diagram of the system, Fig. 2(e), (f), (i) and (j), we can see that each rank of the power spectrum of the system response is reduced in different range. It is also the effect of the random terms in Eq. (1). Additionally, different samples of the random disturbance $\gamma(t)$, simulated from Eq. (2), are substituted into Eq. (1). And the bifurcation diagrams, orbit diagrams, power spectrum diagrams and the Poicare diagrams of the disturbed system calculated with those different samples are approximately invariable.

It is indicated that the samples of the white noise process simulated from Eq. (2) can satisfy the ergodic condition numerically.

Fig. 3 shows the influence of $\Omega$ on the response of the rotor system subject to a white noise process, when $\beta = 0$, $u = 0.1$ and $\Delta K = 0.62$. Here bifurcation diagrams corresponding to a gradual increase of rotating speed

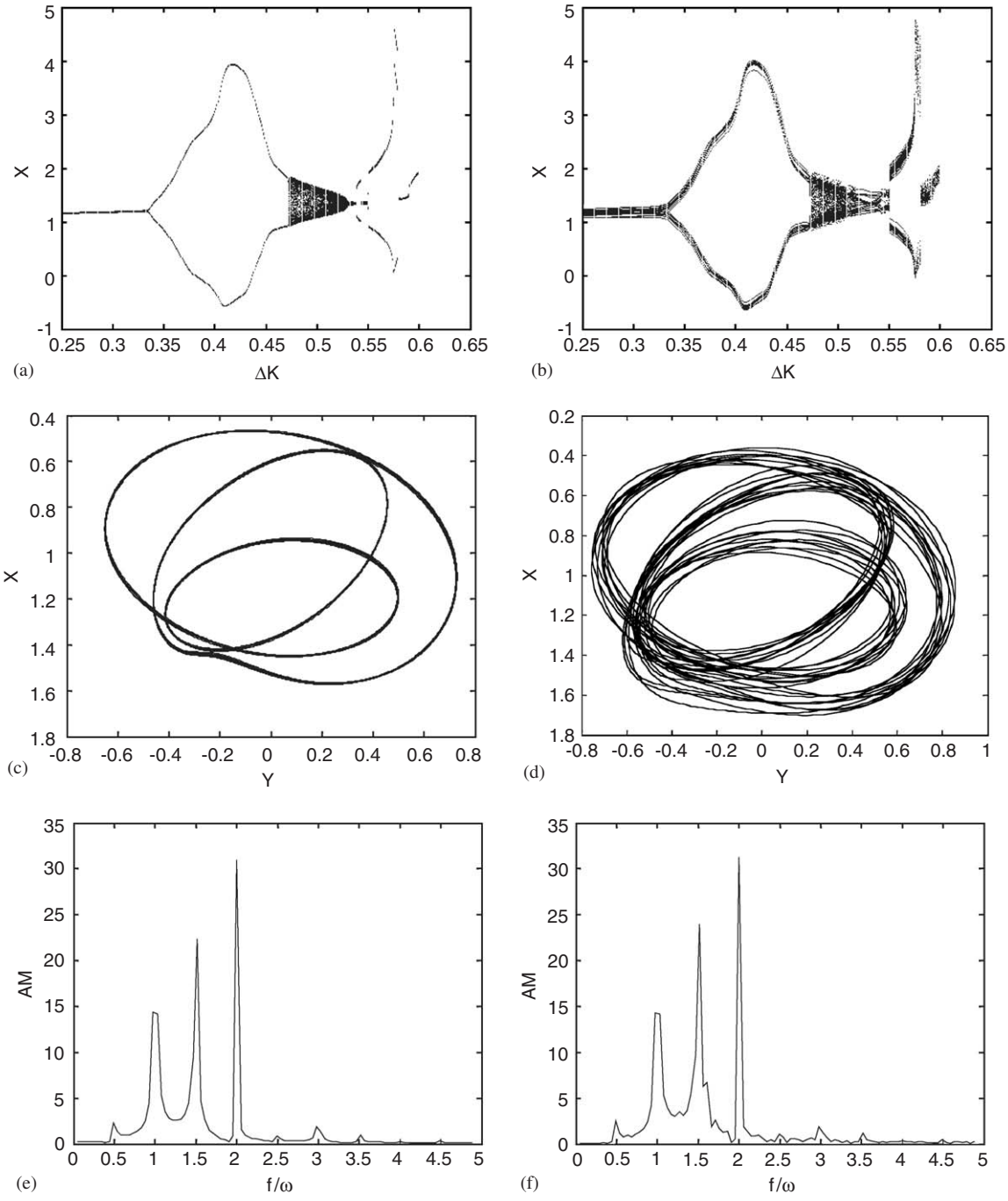


Fig. 2. The influence of $\Delta K$ on system response ($\Omega = 0.56$, $U = 0.1$, $\beta = 0.0$): (a) bifurcation diagram ($\sigma = 0.001$), (b) bifurcation diagram ($\sigma = 0.01$), (c) orbit ($\sigma = 0.001$, $K = 0.35$), (d) orbit ($\sigma = 0.01$, $K = 0.35$), (e) power spectrum ($\sigma = 0.001$, $K = 0.35$), (f) power spectrum ($\sigma = 0.01$, $K = 0.35$), (g) Poincare diagram ($\sigma = 0.001$, $K = 0.5$), (h) Poincare diagram ($\sigma = 0.01$, $K = 0.5$), (i) power spectrum ($\sigma = 0.001$, $K = 0.5$), and (j) power spectrum ($\sigma = 0.01$, $K = 0.5$).

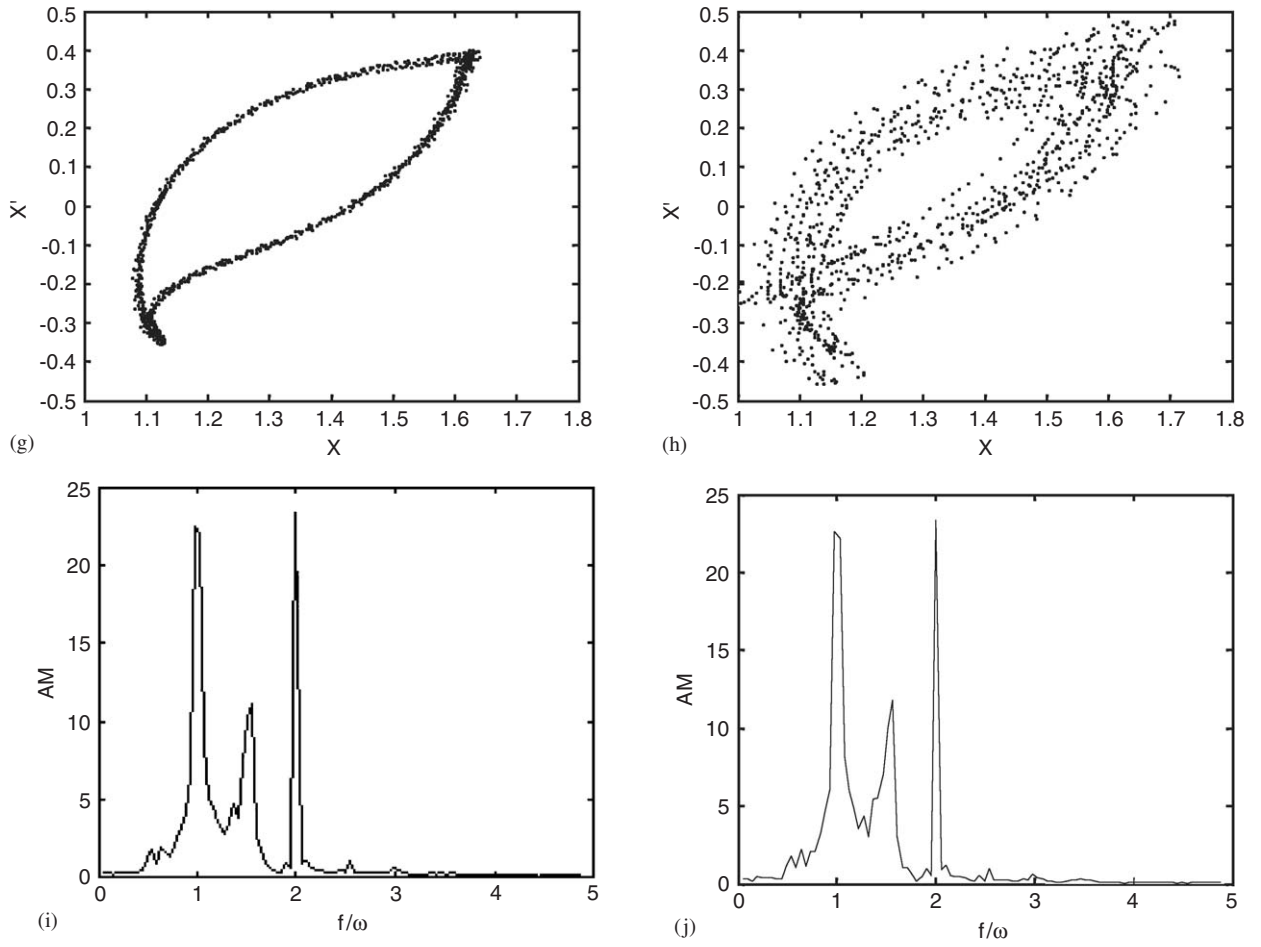


Fig. 2. (*Continued*)

ratio $\Omega$ of the system response are shown in Fig. 3(a) (for the intensity of the random disturbance $\sigma = 0.001$) and Fig. 2(b) (for $\sigma = 0.01$), respectively; Fig. 3(c) and (d) are magnification of Fig. 3(a) and (b); Fig. 3(e) and (f) are undisturbed Poincare diagrams for $\Omega = 0.44$ and 0.535, respectively; Fig. 3(g) and (h) are Poincare diagrams of the system response corresponding to $\Omega = 0.44$, where (g) for $\sigma = 0.001$ and (h) for $\sigma = 0.01$; Fig. 3(i) and (j) are power spectrum diagrams corresponding to 2(g) and (h), respectively; Fig. 3(k) and (l) are Poincare diagrams of the system response corresponding to $\Omega = 0.535$, where (k) for $\sigma = 0.001$ and (l) for $\sigma = 0.01$; Fig. 3(m) and (n) are power spectrum diagrams corresponding to 3(k) and (l); Fig. 3(o) and (p) are Poincare diagrams of the system response corresponding to $\Omega = 0.531$, where (o) for $\sigma = 0.001$ and (p) for $\sigma = 0.01$; and Fig. 3(q) and (r) are power spectrum diagram corresponding to 3(o) and (p), respectively.

From the bifurcation diagrams, Fig. 3(a) and (b), we can see that random disturbance does not influence the bifurcation and chaos characters of the rotor system when $\Omega < 0.52$. When $0.52 < \Omega < 0.525$, the period doubling process from period-1, then to period-3, and finally to chaos, which occurs only in the undisturbed rotor system. From Fig. 3(c) and (d), we can see that the bifurcation cures of periodic two case turn to be thicker one when $0.525 < \Omega < 0.533$, and the higher the random disturbance is, the thicker the bifurcation cures are. Then the solutions of the random disturbed system come into chaotic cases directly as $\Omega > 0.533$. In other words, the period doubling route mentioned above cannot be observed. In fact, as $\Omega$ turns from 0.525 to 0.533, the responses of the system can be the coexistence of random disturbed periodical responses and chaotic responses with different initial conditions. This phenomenon can be observed in Fig. 3(o)–(r). While $\Omega = 0.531$, system response is a disturbed period-3 one for $\sigma = 0.001$, and a chaos one for $\sigma = 0.01$, but in Fig. 3(c) and (d), we can see that the responses of the system is period two case no matter $\sigma = 0.01$ or $\sigma = 0.001$. In addition, from the

power spectrum diagrams, Fig. 3(i), (j), (m) and (n), the frequency component of the disturbed system responses changes obviously, specially when the response of the undisturbed system is a chaos one.

Fig. 4 shows the influence of $\Delta K$ on the response of the rotor system subject to a white noise process, when $\beta = \pi$, $u = 0.2$ and $\Omega$ is near to $2/3\Omega_c$ ($\Omega = 0.6$). Here, the bifurcation diagrams corresponding to a gradual increase of stiffness change ratio $\Delta K$ of the system response are shown in Fig. 4(a) (for the intensity of the

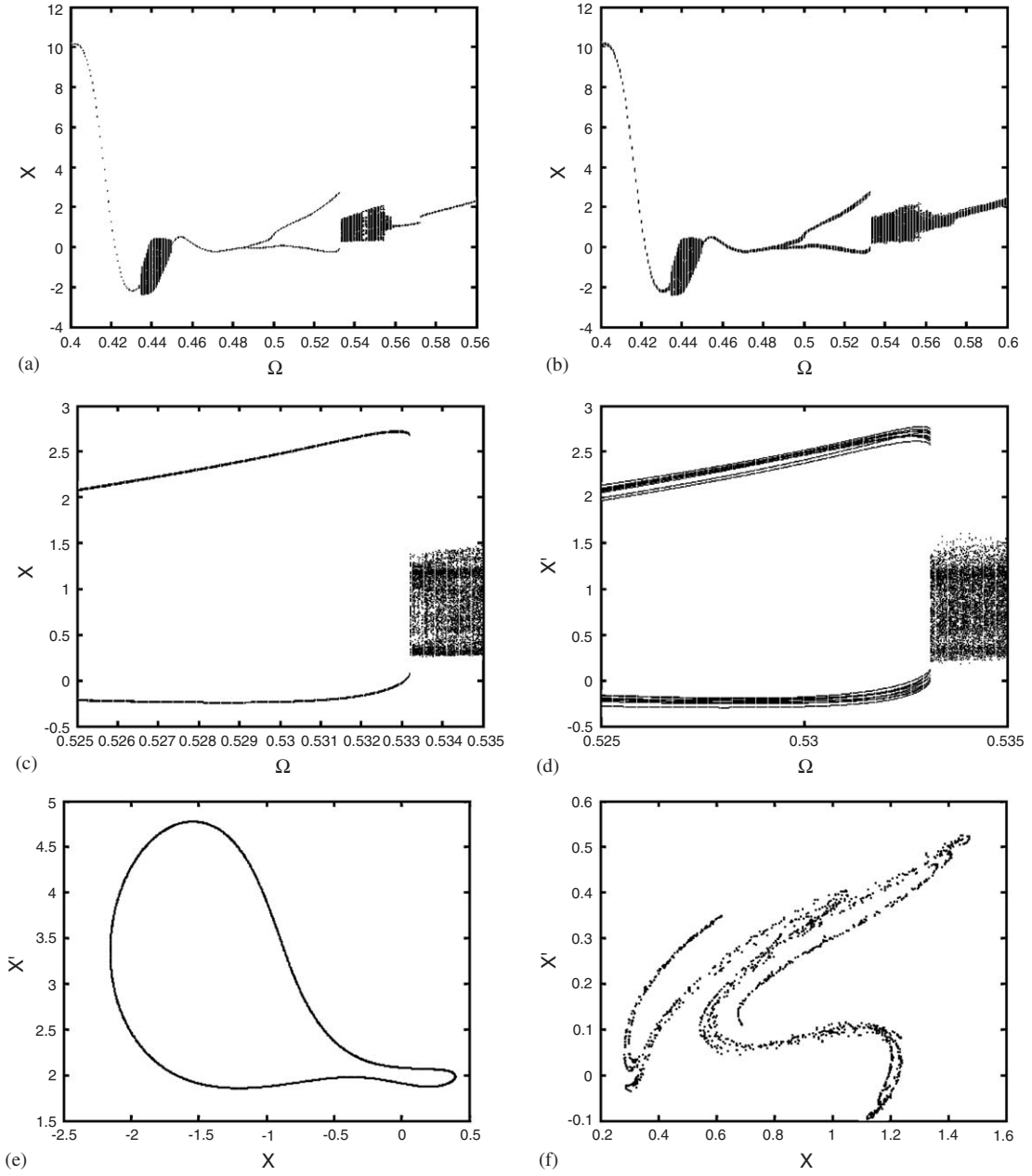


Fig. 3. The influence of $\Omega$ on system response ($U = 0.1$, $\beta = 0$, $\Delta k = 0.62$). (a) bifurcation diagram ($\sigma = 0.001$), (b) bifurcation diagram ($\sigma = 0.01$), (c) magnification of (a), (d) magnification of (b), (e) Poincare diagram ($\sigma = 0.0$, $\Omega = 0.44$), (f) Poincare diagram ($\sigma = 0.0$, $\Omega = 0.535$), (g) Poincare diagram ($\sigma = 0.001$, $\Omega = 0.44$), (h) Poincare diagram ($\sigma = 0.01$, $\Omega = 0.44$), (i) power spectrum ($\sigma = 0.001$, $\Omega = 0.44$), (j) power spectrum ($\sigma = 0.01$, $\Omega = 0.44$), (k) Poincare diagram ($\sigma = 0.001$, $\Omega = 0.535$), (l) Poincare diagram ($\sigma = 0.01$, $\Omega = 0.535$), (m) power spectrum ($\sigma = 0.001$, $\Omega = 0.535$), (n) power spectrum ($\sigma = 0.01$, $\Omega = 0.535$), (o) Poincare diagram ($\sigma = 0.001$, $\Omega = 0.531$), (p) Poincare diagram ($\sigma = 0.01$, $\Omega = 0.531$), (q) power spectrum ($\sigma = 0.001$, $\Omega = 0.531$), and (r) power spectrum ($\sigma = 0.01$, $\Omega = 0.531$).

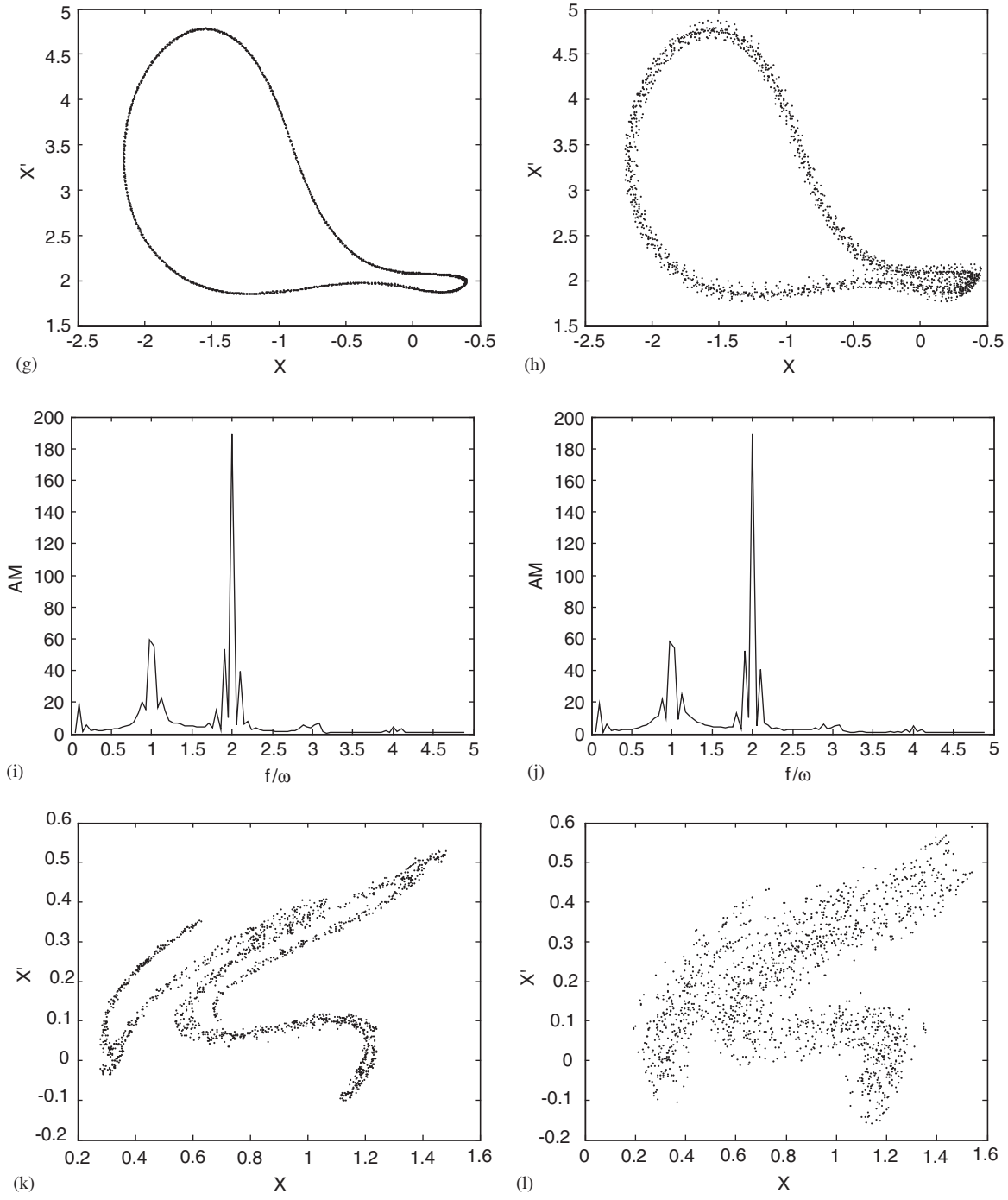


Fig. 3. (*Continued*)

random disturbance $\sigma = 0.001$) and Fig. 4(b) (for $\sigma = 0.01$), respectively; Fig. 4(c) is orbit diagram for $\Delta K = 0.565$, $\sigma = 0.0$ (corresponding to the undisturbed system response); Fig. 4(d) is Poincare diagram for $\Delta K = 0.595$, $\sigma = 0.0$; Fig. 4(e) and (f) are orbit diagrams of the system response corresponding to $\Delta K = 0.565$, where (c) for $\sigma = 0.001$ and (d) for $\sigma = 0.01$, respectively; Fig. 4(g) and (h) are power spectrum diagrams corresponding to 4(e) and (f), respectively; Fig. 4(i) and (j) are Poincare diagrams of the system response

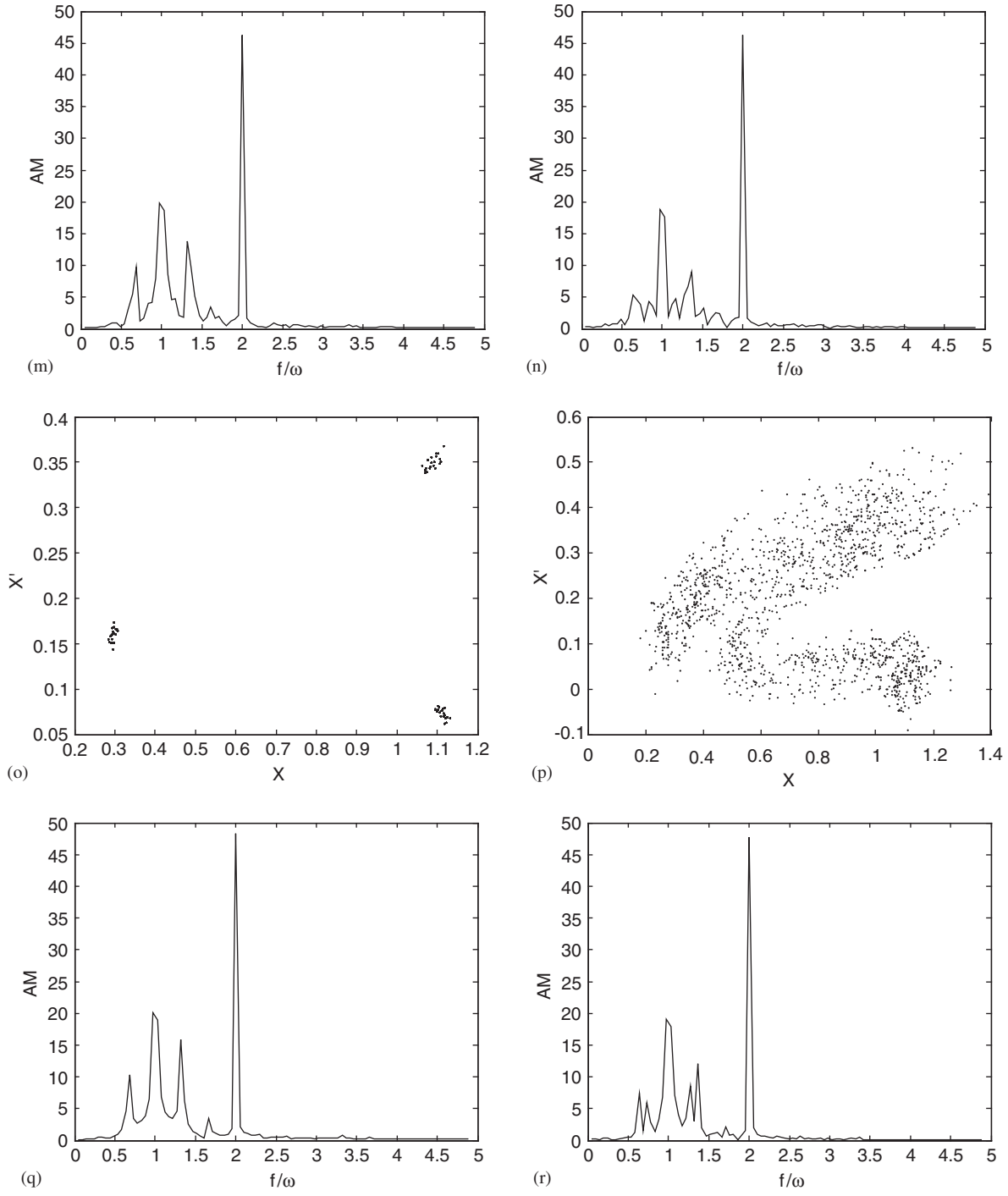


Fig. 3. (*Continued*)

corresponding to $\Delta K = 0.595$, with (i) for $\sigma = 0.001$ and (j) for $\sigma = 0.01$; and Fig. 4(k) and (l) are power spectrum diagrams corresponding to 4(i) and (j).

Compared to the diagrams while the rotor system is undisturbed, from Fig. 4(a), we can see that the bifurcation curves just turn a little thicker, and the bifurcation value of parameter $\Delta K$ is almost invariant. But as we can see in Fig. 4(b), the bifurcation curves are thicker than those in Fig. 4(a), and the bifurcation process

can not be distinguished clearly, when $0.56<\Delta K<0.575$. That is to say, the influence of $\sigma\gamma(t)$ on the response of the rotor system is very weak when its intensity, $\sigma$, is a little one; and such influence turns obviously as $\sigma$ increases. From Fig. 4(e) and (f), we can see that the orbit diagrams, corresponding to $\Delta K = 0.565$, turn to be a family of unclosed curves, which are similar to Fig. 4(c) in its profile. They are also the so-called random disturbed periodical solutions. From the Poincare diagram of the system, Fig. 4(i) and (j) corresponding to

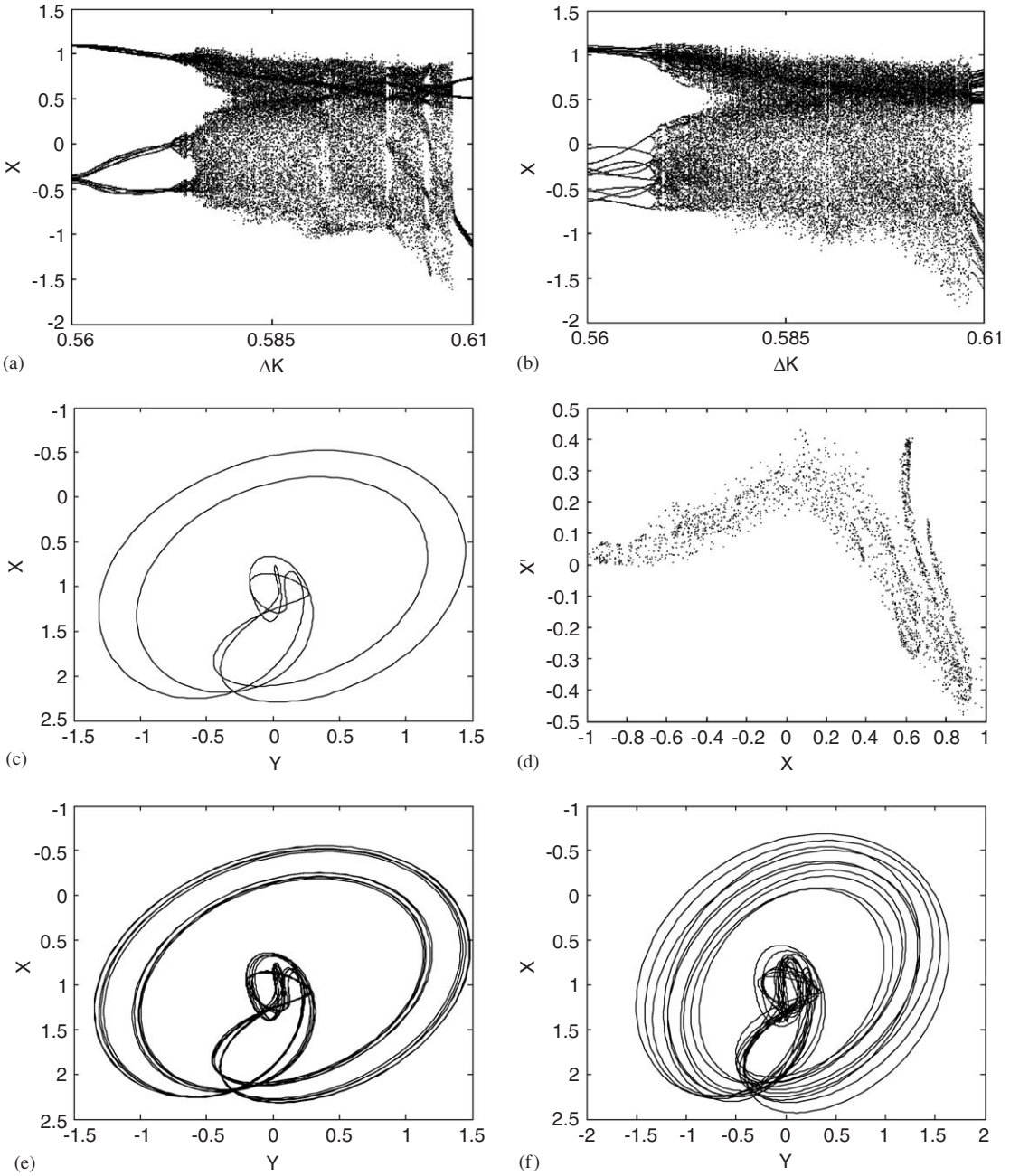


Fig. 4. The influence of $\Delta K$ on system response ($\Omega = 0.60$, $U = 0.2$, $\beta = \pi$). (a) bifurcation diagram ($\sigma = 0.001$), (b) bifurcation diagram ($\sigma = 0.01$), (c) orbit diagram ($\sigma = 0.0$, means without, (d) Poincare diagram ($\sigma = 0.0$, $\Delta K = 0.595$) random disturbance, $\Delta K = 0.565$), (e) orbit diagram ($\sigma = 0.001$, $\Delta K = 0.565$), (f) orbit diagram ($\sigma = 0.01$, $\Delta K = 0.565$), (g) power spectrum ($\sigma = 0.001$, $\Delta K = 0.565$), (h) power spectrum ($\sigma = 0.01$, $\Delta K = 0.565$), (i) Poicare diagram ($\sigma = 0.001$, $\Delta K = 0.595$), (j) Poincare diagram ($\sigma = 0.01$, $\Delta K = 0.595$), (k) power spectrum ($\sigma = 0.001$, $\Delta K = 0.595$), and (l) power spectrum ($\sigma = 0.01$, $\Delta K = 0.595$).

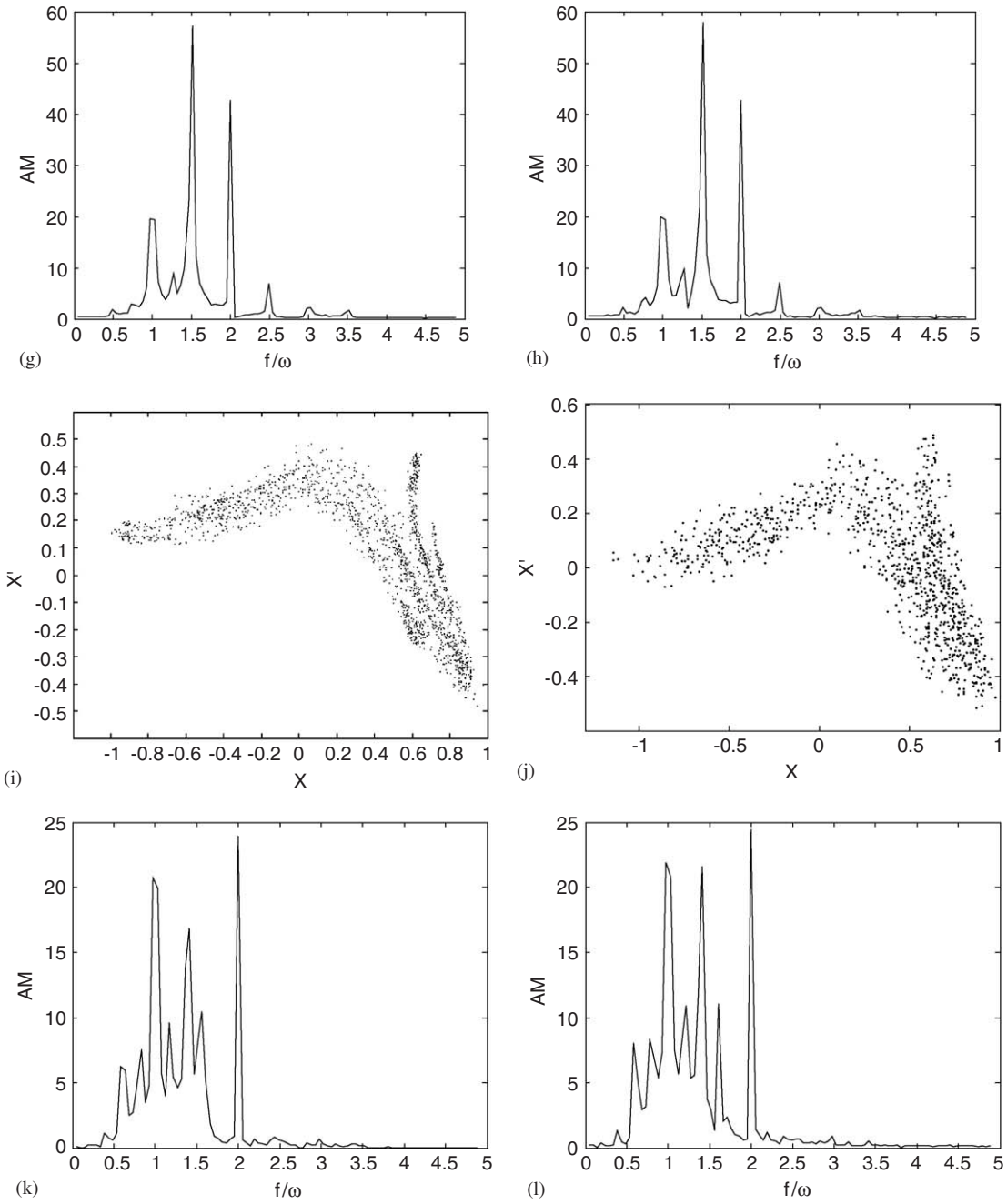


Fig. 4. (*Continued*)

$\Delta K = 0.595$, the so-called random disturbed chaotic solution can be found also. From the power spectrum diagrams of the disturbed system, Fig. 4(e), (f), (i) and (j), we can see that each rank of the power spectrum of the system response is reduced in different range too.

## 4. Summary and conclusion

In this paper, the Monte-Carlo method is applied to investigate the bifurcation and chaos characteristics of a cracked rotor with a white noise process as its random disturbance. Special attention is paid to the influence

of the stiffness change ratio and the rotating speed ratio on the bifurcation and chaos response of the system. Our numerical simulation shows that random disturbance has a significant affect on the system response when the undisturbed response is a quasi-periodic one or a chaos one, and such affect is small when the undisturbed response is a periodical one. Along with the increasing of the random disturbance intensity, the affect mentioned above turns obvious. Additionally, disturbed responses calculated with different samples, which are simulated from Eq. (2), have similar bifurcation diagrams, orbit diagrams, Poincare diagrams and power spectrum diagrams. We expect that the proposed method may become utilizable in the future fault diagnosing of rotating machinery.

## Acknowledgments

The support of the National Natural Science Foundations of China (10325209, 50335030) and China Ph.D. Discipline Special Foundation are greatly acknowledged.

## Appendix A. Some diagrams of the undisturbed case

Some diagrams of the undisturbed case were added in Fig. A1, most of them coming from Zheng and Meng [5,6].

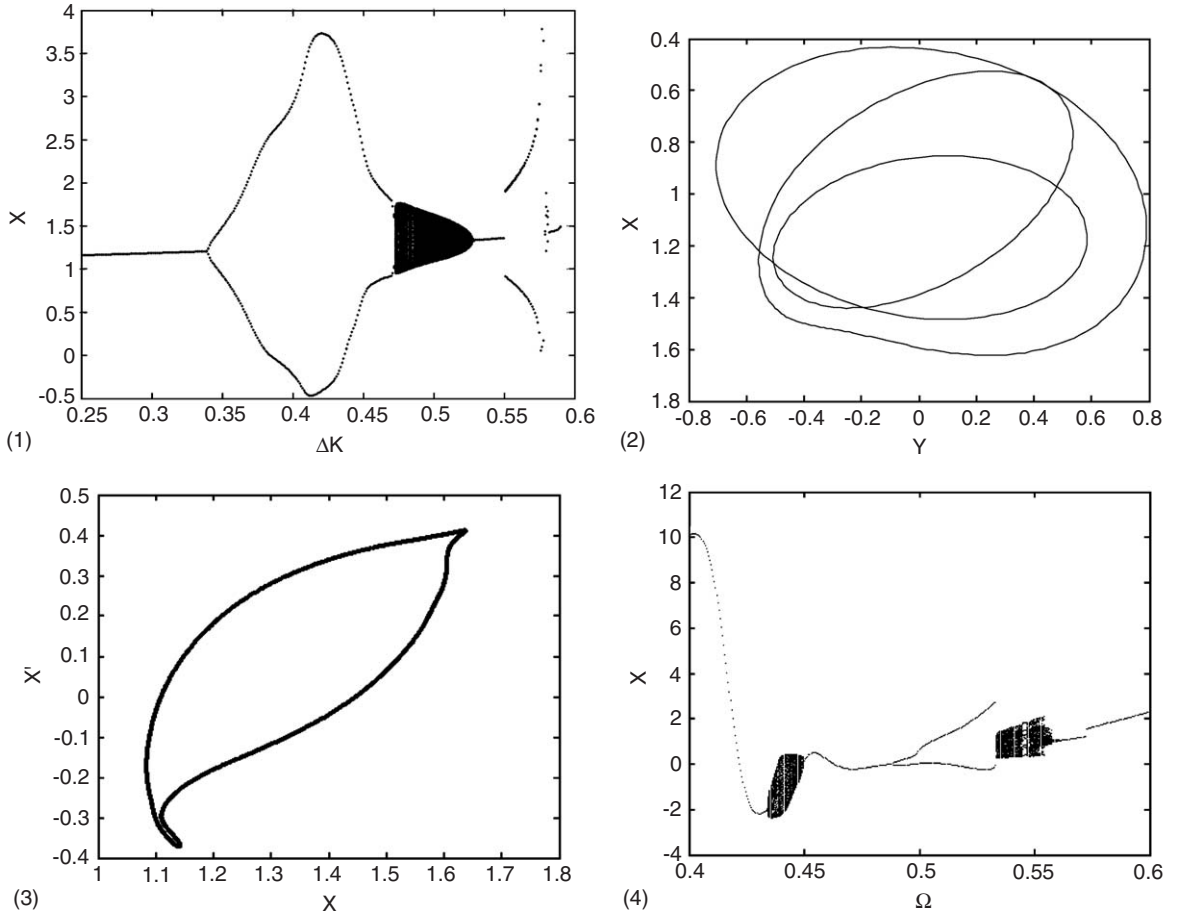


Fig. A1. Some diagrams of the undisturbed cases: (1) bifurcation diagram corresponding to Fig. 2(a) and (b); (2) diagram corresponding to Fig. 2(c) and (d); (3) poincare diagram corresponding to Fig. 2(g) and (h); (4) bifurcation diagram corresponding to Fig. 3(a) and (b); (5) bifurcation diagram corresponding to Fig. 3(c) and (d); (6) poincare diagram corresponding to Fig. 3(o); and (7) bifurcation diagram corresponding to Fig. 4(a) and (b).

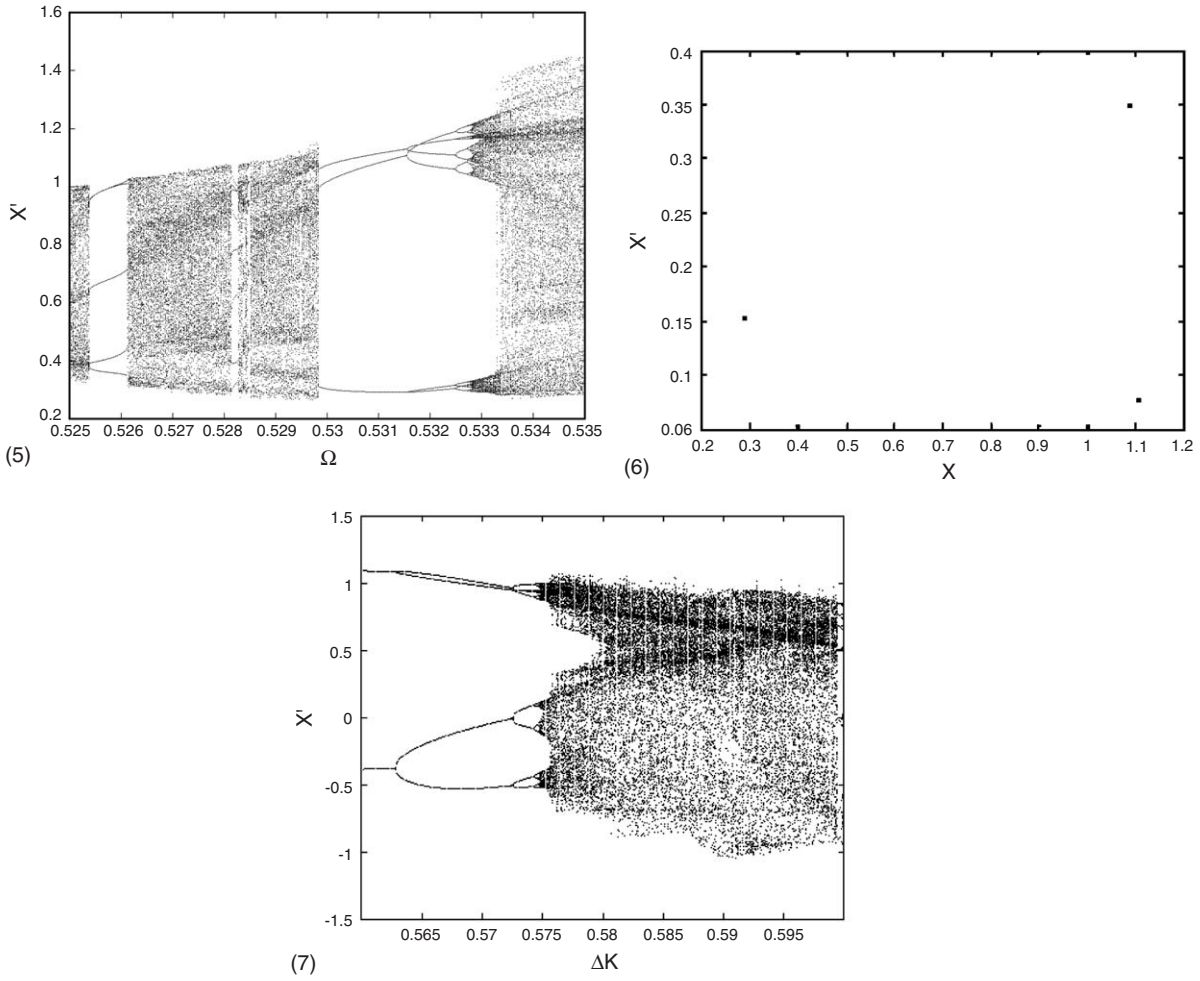


Fig. A1. (*Continued*)

## References

[1] R. Gasch, A survey of the dynamic behavior of a simple rotating shaft with a transverse crack, *Journal of Sound and Vibration,* 162 (1993) 313–332.
[2] J. Gao, X. Zhu, Observation on the dynamic behaviour of cracked rotor, *Chinese Journal of Northwestern Polytechnical University* 10 (1992) 434–439.
[3] A. Muszynska, Shaft crack detection, *Proceedings of the Seventh Machinery Dynamics Seminar*, Edmonton, Canada, 1982.
[4] M. Guang, The nonlinear influence of whirl speed on the stability and response of a cracked rotor, *Journal of Machine Vibration* 4 (1992) 216–230.
[5] Z. Jibing, M. Guang, The Nonlinear influences of whirl speed on bifurcation and chaos of a cracked rotor, *Chinese Journal of Vibration Engineering* 10 (2) (1996) 190–197.
[6] Z. Jibing, M. Guang, Bifurcation and chaos response of a nonlinear cracked rotor, *International Journal of Bifurcation and Chaos* 8 (3) (1998) 597–607.
[7] M. Shinozuka, Simulation of multivariate and multidimensional random processes, *Journal of Sound and Vibration* 19 (2) (1971) 357–367.
[8] M. Shinozuka, Digital simulation of random processes and its applications, *Journal of Sound and Vibration* 25 (1) (1972) 111–128.
[9] Z. Yan, L. Jiahao, Seismic analysis of rotor system under stationary non-stationary random earthquake excitations, *Chinese Journal of Computational Mechanics* 19 (1) (2002) 7–11.